

Chiral Imprinting with Amino Acids of Ordered Mesoporous Silica Exhibiting Enantioselectivity after Calcination

Susana Lacasta,[†] Víctor Sebastián,[†] Clara Casado,[†] Álvaro Mayoral,[‡] Pilar Romero,^{§,||} Ángel Larrea,[§] Eugenio Vispe,^{||,⊥} Pilar López-Ram-de-Viu,^{||,⊥} Santiago Uriel,^{||} and Joaquín Coronas^{*,†}

[†]Departamento de Ingeniería Química y Tecnologías del Medio Ambiente and Instituto de Nanociencia de Aragón, Universidad de Zaragoza, 50018 Zaragoza, Spain

[‡]Laboratorio de Microscopía Avanzada, Instituto de Nanociencia de Aragón, Universidad de Zaragoza, 50018 Zaragoza, Spain

[§]Instituto de Ciencia de Materiales de Aragón (CSIC-Universidad de Zaragoza), 50009 Zaragoza, Spain

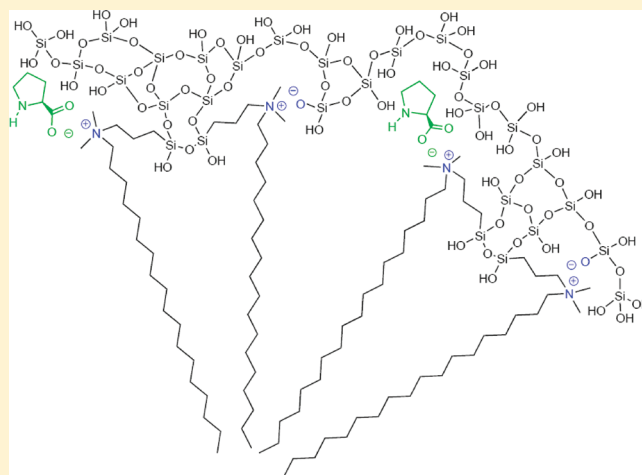
^{||}Departamento de Química Orgánica, Universidad de Zaragoza, 50009 Zaragoza, Spain

[⊥]Instituto Universitario de Catálisis Homogénea (Universidad de Zaragoza-CSIC), 50009 Zaragoza, Spain

S Supporting Information

ABSTRACT: Chiral ordered mesoporous silica (COMS) was synthesized in basic media by combining tetraethyl orthosilicate and quaternized aminosilane (with a templating role) silica sources together with four different standard amino acids (arginine, histidine, isoleucine, and proline). Besides the hexagonal MCM-41-type structure, narrow pore size distribution, and high specific surface area, it was found that these solids have potential for enantiomeric separation because of the transference of chirality from the amino acid to the silica. This is illustrated by the resolution of several racemic mixtures (those of proline, isoleucine, trans-4-hydroxyproline, pipercolic acid, valine, leucine, and phenylglycine) with the calcined COMS prepared with L-proline. The opposite behavior observed in induced circular dichroism experiments with calcined COMS, obtained using both enantiomers of proline, confirmed their chiral nature. The high number and variety of existing amino acids, and chiral organic compounds in general, makes these ordered silicas attractive for the production of enantiopure substances.

KEYWORDS: amino acids, chirality, chiral resolution, sol–gel processes, ordered mesoporous silica, zeolite analogue



1. INTRODUCTION

Because of their uniform pore sizes within the range of a few nanometers and their large surface areas, ordered mesoporous silica complement conventional zeolites in applications related to adsorption,¹ catalysis,² drug delivery,³ tissue engineering,⁴ membranes,⁵ and sensing,⁶ among others. Most mesoporous materials (e.g., MCM-41 and MCM-48) have been synthesized at high pH by templating with cationic surfactants.⁷ Anionic and nonionic surfactants have also attracted interest as templates for mesoporous materials. Their interaction with silica precursors generally needs to be enabled by the use of either low pH (SBA-15, SBA-16),^{8,9} to reverse the silica charge, or a positively charged silica source, such as aminosilane or quaternized aminosilane, acting also as a structure-directing agent.^{10,11}

The availability of an inexpensive and robust porous chiral silica-based solid could help the development of enantioselective

adsorption separations as a feasible alternative to other existing approaches.^{12,13} Chiral microporous solids such as certain zeolites¹⁴ would not have pores large enough for treating molecules of relatively large size. Other (helical) mesostructured materials recently reported exhibit chirality (in terms of the length of one complete helix turn) on a scale about 2 orders of magnitude larger than the mesopore size and, hence, do not show chiral separation performance.¹⁵ Furthermore, the external morphology of twisted rods reported several times is not a direct indication of chiral pore structure, which is also difficult to determine unambiguously from TEM imaging.¹⁶

Received: November 12, 2010

Revised: January 5, 2011

Published: January 21, 2011

Amino acids are pH-sensitive zwitterionic surfactants compatible with all other types of surfactants, in some cases less soluble in water and often insoluble in most organic solvents, including ethanol. As they are ampholytic compounds, they display the properties of anionics at high pH. Recently, amino acids have been employed as proton providers for exchanging porous layered silicate in mild conditions¹⁷ and for buffering the synthesis of dodecasil 3C.¹⁸ Concerning the production of nanoporous materials, ordered silica structures have been obtained by the self-assembling of synthetic cysteine–lysine block copolypeptides that mimic the properties of silicatein, producing the hydrolysis and aggregation of tetraethoxysilane,¹⁹ while an anionic surfactant based, among others, on the amino acid alanine (N-myristoyl-L-alanine sodium salt) has templated the synthesis of mesoporous silica.^{11,20,21} In an attempt to achieve biomimetic silicification, homopeptides [poly(lysine) and poly(arginine)] have been shown to induce the formation of mesoporous silica.²² To understand the contribution of complex components (proteins) in biosilicification, several amino acids have been directly studied in their role as silica polymerizing agents at pH 7.^{23,24} In addition, nanoparticles have been found in unbuffered lysine–silica sols,²⁵ i.e., in conditions of high pH common to those employed for templating mesoporous silica, while periodic arrangements of silica nanospheres have been produced through a modification of the so-called Stöber method using basic amino acids (L-lysine or L-arginine) instead of ammonia.²⁶

In the present work, chiral ordered mesoporous silica (COMS) has been prepared by hydrothermal synthesis at high pH, in the presence of the amino acids L-arginine, L-histidine, L-isoleucine, and L-proline, and quaternized aminosilane N-3-[3-(trimethoxysilyl)propyl]-N-octadecyl-N,N-dimethylammonium chloride (C₁₈-TMS) and tetraethyl orthosilicate (TEOS) as silica sources, followed by calcination. This COMS, as shown below, has the same 2-D hexagonal structure as MCM-41 ordered mesoporous silica prepared with cetyltrimethylammonium (CTA) surfactant.⁷ However, our COMS does not lose enantioselectivity upon calcination, in contrast to non-ordered enantioselective sol–gel materials.²⁷ For instance, chiral sol–gel imprinted materials obtained with chiral cationic surfactant lose enantioselectivity upon calcination.^{28,29}

2. MATERIALS AND METHODS

Synthesis of Chiral Ordered Mesoporous Silica. Silica mesoporous powders were prepared using tetraethyl orthosilicate (TEOS, 98 wt %, Aldrich) as the main Si source and the quaternized silicon source, N-3-[3-(trimethoxysilyl)propyl]-N-octadecyl-N,N-dimethylammonium chloride (C₁₈-TMS, 50 wt % in methanol, Flourochem) as initiator, in the presence of several amino acids: L-arginine (98 wt %, Aldrich), L-histidine and L-isoleucine (both, 99 wt %, Aldrich), and L-proline (99 wt %, Fluka). The molar composition was TEOS:C₁₈-TMS:amino acid:H₂O:NaOH = 6:1:2:1000:4. Typically, 54 g of a precursor gel containing L-proline was prepared by adding 0.605 g of amino acid, 2.637 g of C₁₈-TMS, and 3.337 g of TEOS to 0.423 g of NaOH (99 wt %, Aldrich) and 47.58 g of H₂O, in that order, and stirred at room temperature to homogeneity. The pH measured then had a value of 10.8–11.0. This value was approximately the same at the end of the synthesis. Because a cloudy dispersion was quickly produced once the reactants were mixed at room temperature, it can be deduced that the hydrolysis of both TEOS

and C₁₈-TMS is fast enough to not control the formation of the final solid. The resulting mixture was maintained at 80 °C for 24 h. The product was then washed, filtered, and dried at 80 °C overnight. Around 0.6 g of the product was recovered after drying. The organic material was removed by calcination at 650 °C for 8 h with a heating rate of 10 °C/min. For comparison purposes, samples were prepared with DL-amino acids: DL-proline (99 wt %, Alfa Aesar), DL-isoleucine (99 wt %, Aldrich), DL-histidine (99 wt %, Aldrich), DL-arginine (97 wt %, Aldrich), and D-proline (99 wt %, Aldrich).

Characterization. The ordered mesoporous materials obtained were analyzed by powder small angle x-ray diffraction (SA-XRD) in a Philips X'Pert diffractometer with Bragg–Brentano geometry and Cu K_α (40 kV, 20 mA) radiation. Thermogravimetric analyses were performed using Mettler Toledo TGA/SDTA 851^e equipment. Samples (10 mg) placed in 70 μL alumina pans were heated in air flow up to 900 °C at a heating rate of 10 °C/min. After degassing at 200 °C for 10 h, N₂ adsorption/desorption isotherms were obtained using a Micromeritics Tristar 3000 surface area and porosity analyzer. The specific surface area was calculated according to the BET method (in the 0.05–0.25 range of relative pressure). The corresponding pore volumes and pore size distributions were calculated from the adsorption and desorption branches using the BJH approach.

After calcination, selected samples were ultrasonically dispersed in acetone, placed on lacey carbon-coated copper grids, and subsequently observed at 200 kV in a JEOL-2000 FXII TEM and at 300 kV on a TECNAI F30, point resolution 1.7 nm, and Cs 1 mm.

Solid-state NMR experiments were performed on a Bruker Avance 400 spectrometer, operating at frequencies of 400.13 MHz for ¹H, 100.61 MHz for ¹³C, and 79.41 for ²⁹Si. Data were acquired at 23 °C and chemical shifts referenced to TMS (tetramethylsilane). A double resonance (¹H-X) probe with a 4 mm rotor diameter was used, and the spinning frequency was set to 8 kHz. The ¹H 90° pulse length was 5.1 μs, and the CP contact time was set to 1.5 and 9 ms for ¹³C and ²⁹Si CPMAS, respectively. The recycle delay was 5 s, and the pulse sequence employed consisted of ramped cross-polarization with TPPM (two-pulse phase-modulated) decoupling.

NMR experiments in solution were recorded using standard pulse sequences on a Bruker Avance 500 spectrometer operating at 500.13 MHz for ¹H and at 125.7 MHz for ¹³C. The spectra were measured in D₂O solutions at 25 and 40 °C. Chemical shifts are given in ppm relative to TMS, and the solvent residual peak was used as internal standard.

The ¹H-¹³C HSQC spectrum was used in conjunction with the ¹H-NOESY spectrum to complete the assignments of the resonances. Mixing time (between 0.6 and 1 s) was optimized by ¹H T1 measurements, and the relaxation delay was 2 s. ¹H NMR diffusion measurements (DOSY) were performed using a stimulated echo sequence with bipolar gradient pulses (BPLED). Diffusion time (τ) was set to 250 ms. The pulsed gradients were incremented from 2% to 95% of the maximum strength in 16 spaced steps with a duration (δ/2) of 2.2–3 ms.

The Raman scattering spectra of calcined solids were recorded with a dispersive Raman spectrophotometer JASCO NRS-3100. Raman spectra were collected from neat solid samples, excited with a 785 nm laser to minimize the fluorescence background. The laser power was set between 100 and 200 mW, depending on the fluorescence observed in the samples. The Raman data were collected over the 400–1400 cm⁻¹ range at a spectral band-pass

Table 1. Synthesis of Chiral Ordered Mesoporous Silica (COMS) at 80 °C for 24 h Using TEOS:C₁₈-TMS:L-AA:H₂O:NaOH = 6:1:2:1000:4^a

| sample | amino acid | S _{BET} (m ² /g) | BJH pore size (nm) | | BJH pore volume (cm ³ /g) | |
|------------|--------------|--------------------------------------|--------------------|------|--------------------------------------|------|
| | | | Ads. | Des. | Ads. | Des. |
| L-Arg-COMS | L-arginine | 1029 | 3.2 | 3.2 | 0.99 | 0.99 |
| L-His-COMS | L-histidine | 1130 | 3.2 | 3.3 | 1.02 | 1.13 |
| L-Ile-COMS | L-isoleucine | 840 | 3.3 | 3.2 | 0.83 | 0.83 |
| L-Pro-COMS | L-proline | 1010 | 2.9 | 2.8 | 0.80 | 0.80 |
| blank | — | 1336 | 3.9 | 4.2 | 0.66 | 0.62 |

^a AA refers to Arg (arginine), His (histidine), Ile (isoleucine), and Pro (proline). The textural properties were analyzed in samples calcined at 650 °C for 8 h. The blank sample did not yield the MCM-41-type structure.

of 2 cm⁻¹. Multiple scans (30–50) were averaged to improve signal-to-noise ratio. In the cases where strong background scattering made analysis difficult, a sloping spline baseline was subtracted from the spectrum. Polarization experiments were carried out on the same spectrophotometer using a Thermoscan zinc selenide P/N 0014–051 polarizer as analyzer.

Induced circular dichroism (ICD) experiments were carried out on calcined COMS samples (20 mg) treated at room temperature with 5 mM phenol in methanol solution (0.4 mL) for 10 h. The dispersion was then centrifuged to remove excess phenol, and the slurry was left to dry overnight at room temperature to yield the solid on which circular dichroism (CD) was measured. Solid-state CD spectra were generated from disks produced pressing a solid obtained from the grinding of KBr (15 mg) together with the solid sample (10 mg). The spectra were recorded on a Jasco J-810 spectropolarimeter over the 250–300 nm wavelength range.

Separation of Racemates. The calcined chiral ordered mesoporous solids (COMSs) were studied in selective adsorption of amino acid experiments. Most of the racemic amino acids were used as purchased to prepare solutions in distilled water: DL-proline (99 wt %, Alfa Aesar) *c* = 10 mg/mL, DL-isoleucine (99 wt %, Aldrich) *c* = 4 mg/mL, DL-histidine (99 wt %, Aldrich) *c* = 10 mg/mL, DL-arginine (97 wt %, Aldrich) *c* = 10 mg/mL, DL-pipecolic acid (99 wt %, Aldrich) *c* = 10 mg/mL, DL-valine (99 wt %, Aldrich) *c* = 4 mg/mL, DL-leucine (99 wt %, Aldrich) *c* = 4 mg/mL, and DL-2-phenylglycine (99 wt %, Aldrich) *c* = 2 mg/mL. Solutions of racemic trans-4-hydroxyproline (*c* = 10 mg/mL) were prepared by mixing the same quantity of L-trans-4-hydroxyproline (99 wt %, Aldrich) and D-trans-4-hydroxyproline (99 wt %, Aldrich). In such conditions, amino acids are mainly in their zwitterionic form (i.e., bearing zero overall charge). Samples of the studied COMSs (40 mg) were shaken for 1 week with the corresponding solutions of rac-AA (2 mL of rac-Pro, rac-His, rac-Arg, rac-Hyp, and rac-pipecolic acid solutions, 5 mL of rac-Ile, rac-Val, and rac-Leu solutions, and 10 mL of rac-Phg solution, respectively). Afterward, the suspensions were left to settle and the supernatant solutions analyzed by HPLC-ESI-MS.

HPLC-ESI-MS was carried out using an Agilent 1100 HPLC system equipped with an autosampler G1367A and a quaternary pump G1311A. The MS detector connected to the Agilent system was a Bruker Esquire 3000 plus quadrupole ion trap mass spectrometer equipped with electrospray. The HPLC analytical assays were carried out on a 250 mm × 4.6 mm ID Chirobiotic T column (Astec, Inc.). All analytical assays were performed at a flow rate of 1.2 mL/min, using as eluent a mixture of 60/40 methanol/water composition acidified by acetic acid (0.0125%). The solutions for analysis were obtained by dilution

of the shaken solutions with the corresponding COMS. The dilution factor was different for starting and adsorbed amino acid solutions: 1000 times for starting solutions and 500 times for adsorbed solutions. Injection volume was, in all cases, 5 μL. In all cases, both starting and adsorbed amino acid solutions were analyzed at the same time to obtain reference values. The D/L-AA separation factor ($\alpha_{D/L}$) was calculated as the quotient between the ratio of the fractions of D-AA and L-AA in the solution in contact with the corresponding COMS for 1 week to that in the starting racemic solution.

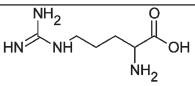
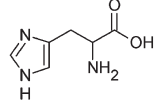
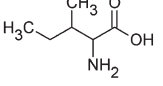
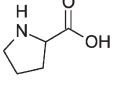
3. RESULTS AND DISCUSSION

Table 1 shows the synthetic conditions and results for the preparation of the four different COMSs. Note that C₁₈-TMS, besides a silica source, is also a cationic surfactant, which also plays the role of conventional CTA cation.⁷ The structural formulae and selected properties of the present amino acids are listed in Table 2. The basic conditions used guarantee the fast hydrolysis of TEOS and C₁₈-TMS quaternized silica to yield hydrophilic silicate monomers. At the high working pH of about 11, the amino acids tested were in the anionic form, with the exception of arginine (pK_{a3} = 12.48, see Table 2). The charge matching between organic surfactant and inorganic silicate components established in the case of the hydrothermal synthesis of MCM-41 and SBA-15¹⁵ can also be applied to C₁₈-TMS and the corresponding amino acid. In fact, there is amino acid excess with respect to the surfactant.

However, as illustrated in Figure 1 (the mechanism that we hypothesize), there are important differences between the conventional synthesis of MCM-41 using a CTA cation and the syntheses carried out here combining C₁₈-TMS surfactant and amino acids:

- The possibility of condensation between hydrolyzed C₁₈-TMS surfactant molecules to produce dimers (the formation of trimers or tetramers is not considered for simplicity).
- The possibility of organization of the aminosilane dimers into micelles, where the amino acid molecules could electrostatically interact with the positively charged C₁₈-TMS dimers. This electrostatic interaction would compete with that established between the micelle and the negatively charged silica species (because of the basic pH).
- The reaction of hydrolyzed C₁₈-TMS surfactant molecules having silanol groups with silicate species via covalent bonds. This means that the binding energy of the organic–inorganic interphase would be much larger than in the

Table 2. Selected Properties and Structural Formulae of the Amino Acids Used in this Work for the Synthesis of COMS

| Amino acid (AA) | pK _{a1} (-COOH) | pK _{a2} (-NH ₃ ⁺) | pK _{a3} (side chain) | Hydropathy index | Structural formula |
|------------------|--------------------------|---|-------------------------------|------------------|--|
| Arginine (Arg) | 2.17 | 9.04 | 12.48 | -4.5 |  |
| Histidine (His) | 1.82 | 9.17 | 6.00 | -3.2 |  |
| Isoleucine (Ile) | 2.36 | 9.68 | - | 4.5 |  |
| Proline (Pro) | 1.99 | 10.96 | - | 1.6 |  |

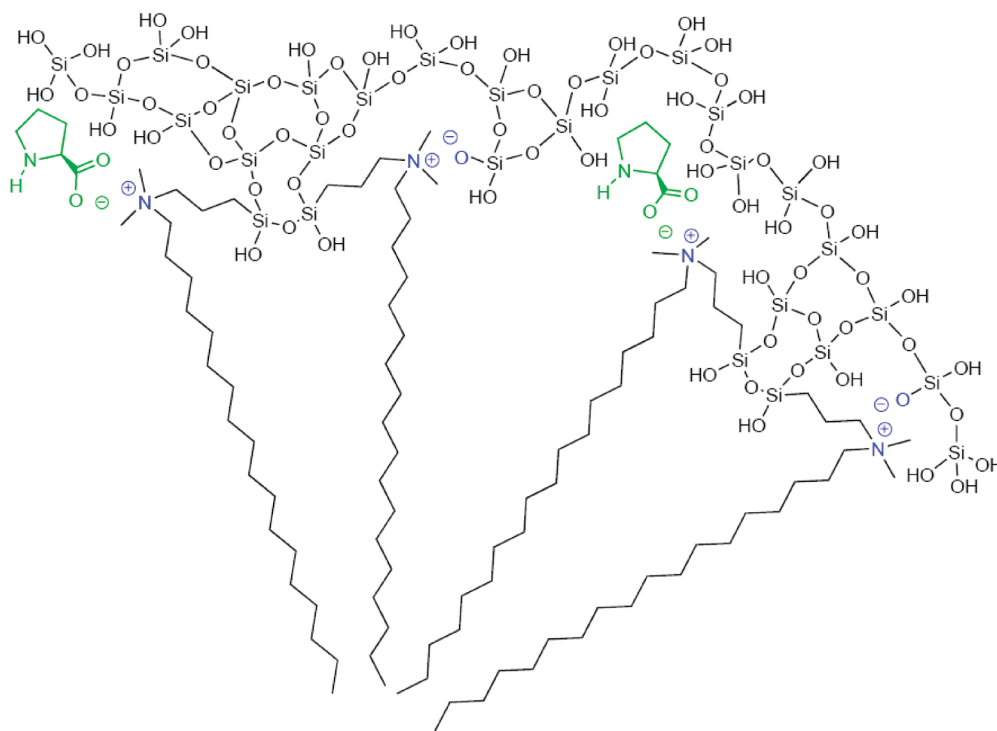


Figure 1. Sector of the suggested micelle constituted by alternating C₁₈-TMS dimers and amino acid (proline) molecules or negatively charged silica species. The organization of the aminosilane dimers into micelles serves as a template for the formation of the ordered mesoporous silica, while the amino acid transfers its chirality to the micelle and from there to the silica.

conventional synthesis of MCM-41, where the interaction between silicates and CTA is only electrostatic.

The ²⁹Si CP-MAS NMR (Figures S1A and S1B of the Supporting Information) confirms the functionalization of the mesoporous silica obtained here by the covalent bonding with the C₁₈-TMS surfactant. Besides the typical Q², Q³, and Q⁴ silica environments, T² and T³ sites (signals centered at -60 and -68 ppm), assigned to (-SiO)₂SiOH(-CH₂) and (-SiO)₃Si(-CH₂), respectively, were observed.

The micelle constituted by alternating C₁₈-TMS dimers and amino acids or negatively charged silica species makes possible

the efficient transference of chirality to the ordered mesoporous silica in a mechanism where the amino acid leaves its molecular imprint in the silica. The electrostatic character of the interaction with the amino acid was corroborated by DOSY and NOESY NMR experiments³⁰ that did not evidence the presence of the chiral molecules inside the micelle. This means either the amino acids are not occluded in the hydrophobic part of the micelle or their quantitative presence is below the detection limit of the technique (around 0.1%). In addition, this suggests that only a small amount of amino acid would be responsible for the transference of chirality to the silica. The presence of a chiral

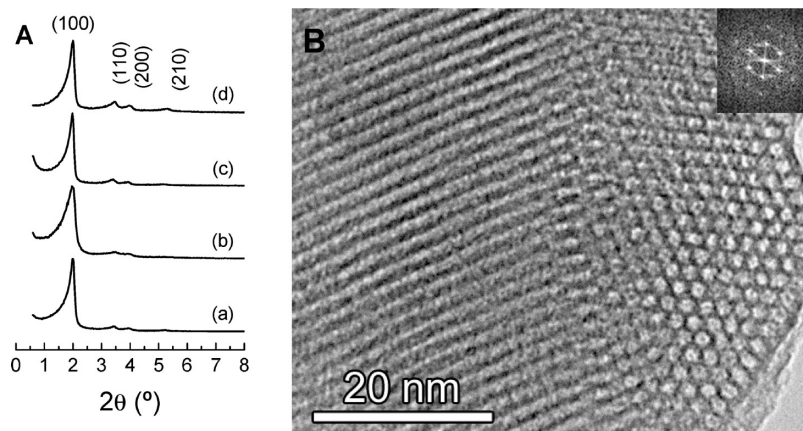


Figure 2. Low-angle XRD patterns of uncalcined ordered mesoporous silicas prepared with L-amino acids (A): L-Arg-COMS (a), L-His-COMS (b), L-Ile-COMS (c), and (d) L-Pro-COMS. (B): TEM image of a grain of L-Ile-COMS showing the pores hexagonally arranged, the inset being the Fourier transform.

molecule³¹ may not be a sufficient condition for obtaining the chiral silica. In fact, this is an indispensable condition together with the covalent bonding between the micelle and the silica precursor.

Having established the main differences between the preparation of our COMS and common ordered mesoporous silica (e.g., MCM-41), Figure 2A shows that the materials synthesized in the presence of the amino acids L-Arg, L-His, L-Ile, and L-Pro, TEOS, and the surfactant C₁₈-TMS are periodic mesoporous silica. All the XRD patterns show four peaks: one strong peak in the 2.0–2.1° 2θ interval and three additional weak peaks at 3.4–3.6°, 3.9–4.1°, and 5.2–5.4° 2θ values. These peaks are compatible with the hexagonal structure of MCM-41, and hence, they can be indexed to (100), (110), (200), and (210) with a lattice parameter of 4.2–4.4 nm.⁷ The structure of MCM-41 is formed by cylindrical pores hexagonally arranged. In addition, because all of the XRD patterns exhibit narrow (100) peaks and separated small reflections, a high degree of structural order can be attributed to the new silica materials reported here. The samples keep their XRD order upon calcination (Figure S2 of the Supporting Information), even though the mesoporous ordering was somehow affected.

Electron diffraction experiments in the TEM confirmed the presence of very weak diffraction spots near the intense central unscattered spot, as expected from an ordered mesoporous material constituted by walls of amorphous silica. Panel B of Figure 2 displays the high resolution TEM image of the material, showing the channels perpendicular to the electron beam and the hexagonal arrangement on the edge of the crystal. After tilting several crystals, no other arrangement was found confirming the hexagonal symmetry of the material. The FFT shown in the inset was indexed assuming *p6mm* symmetry, obtaining a unit cell value of 4.2 nm, in good agreement with the XRD experiments, and the pore size 2.5 nm, within about 10% of accuracy. Figure S3 of the Supporting Information shows similar features for COMS prepared with the other three amino acids.

As shown in Table 1, the ordered mesoporous silica obtained possesses BJH pore sizes in the 2.8–3.3 nm range with BET specific surface areas as high as 1130 m²/g (sample L-His-COMS). The relatively small pore size obtained here can be linked to the low synthesis temperature of 80 °C. In fact, the mesoporous size is affected by synthesis time and temperature

and silica and surfactant concentrations, among others. In particular, in the case of MCM-41 materials, a low-temperature synthesis (100 °C) yielded BJH pore sizes in the 3.1–4.2 nm range, whereas using a high temperature (165 °C) larger pores have been obtained (4.7–5.1 nm).³² For all the samples obtained here a sharp increase in the volume adsorbed is observed at relative pressures from 0.2 to 0.5 in the corresponding type IV isotherms (Figure S4 of the Supporting Information). This increment is attributed to nitrogen capillary condensation in the mesoporosity of the ordered silica, while the sharpness of the inflection agrees with the uniformity and narrowness (0.5–0.7 nm peak widths at half-maxima) of the unimodal pore size distribution (see the inset in Figure S4 of the Supporting Information).³² The absence of hysteresis is consistent with pore diameters below approximately 4 nm.³³ AMS-type ordered mesoporous silica materials obtained in the presence of anionic surfactants with C₁₂–C₁₆ aliphatic chains and quaternized aminosilane exhibited only BET surface areas in the 370–600 m²/g range,²⁰ in some cases with broad pore size distribution.¹¹

To gain insight into the microstructure of our calcined COMS, Raman spectra were recorded for samples prepared in the presence of L- and DL-amino acids (L-AA-COMS and DL-AA-COMS, respectively; AA refers to Arg, His, Ile, and Pro). A typical Raman spectrum of these solids (Figure S5 of the Supporting Information) is similar to those of other ordered mesoporous materials.^{34,35} In consequence, the observed bands are assigned to three- and four-membered rings (cyclic siloxanes) (at 505 and 615 cm⁻¹, respectively) to mixed modes of bending and symmetric stretching of siloxane bridges (Si–O–Si) and surface silanol groups (–Si–OH) (at 760–850 and 985 cm⁻¹, respectively) and to asymmetric stretching siloxanes (at 1070–1125 cm⁻¹). Moreover, well-resolved peaks in the 760–850 cm⁻¹ range are similar to the peaks described for highly ordered structures such as silicalite-1 or coesite.³⁶

In addition, polarized Raman scattering measurements were carried out to explore the degree of anisotropy as has already been done in other materials such as carbon nanotubes or polyamide fibers.^{37–39} Polarization properties of Raman scattered light allow measurements to be made in parallel and perpendicular planes with respect to the incident polarized light, and as a result, the spectrum intensity in both planes should be as

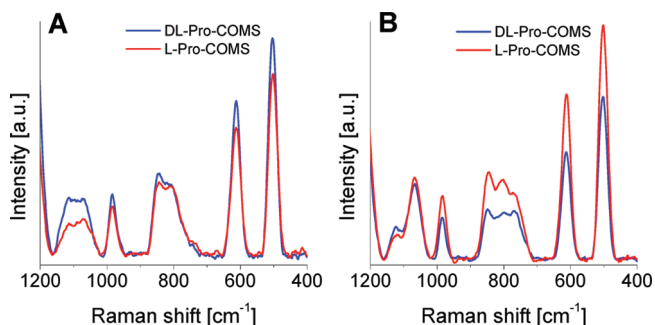


Figure 3. Polarized perpendicular (A) and parallel (B) scattered Raman spectra of calcined *L*-Pro-COMS and *DL*-Pro-COMS.

different as the anisotropy of the vibrations and hence of the material. Figure 3 shows the perpendicular (3A) and parallel (3B) scattering for *L*-Pro-COMS and *DL*-Pro-COMS. It can be inferred that *L*-Pro-COMS produces higher intensity differences than its racemic parent, as corresponds to a chiral environment. This behavior can be observed to a lesser degree in *L*-His-COMS but not in *L*-Arg-COMS, for which the Raman scattering is close to that of *DL*-Arg-COMS (Figure S6 Supporting Information). These results point to an extra intrachannel order in some of our silica materials that must be somehow related to their functional chirality.

On the basis of the hypothesis of transference of chirality from the *L*-amino acid used to the silica produced, the observed textural properties together with the regular mesostructure and the special features evidenced by Raman spectroscopy suggest the possibility of applying the synthesized silica materials to resolving enantiomeric mixtures. This is something of paramount importance in the drug delivery research field. Because of the stereospecificity of biological effects, a great number of medicinal agents are chiral molecules, and their physiological activity may depend on their absolute configuration (sometimes one of the enantiomers is active, whereas the other has no effect or, even worse, has undesired effects).

In these circumstances, calcined COMSs have been tested in enantioselective adsorption experiments. Samples of the four studied COMSs were stirred with the corresponding solutions of racemic Pro, Ile, His, or Arg in their zwitterionic form (which is more convenient for adsorption from aqueous solutions⁴⁰), and the solutions were then analyzed. The more significant enantiomeric separation factors ($\alpha_{D/L}$) achieved are shown in Figure S7 of the Supporting Information: adsorption of each racemate on the corresponding *L*-AA-COMS, adsorption of racemic proline on all the *L*-AA-COMS, and adsorption of all the racemic amino acid solutions on *L*-Pro-COMS. The rest of the experiments (not depicted) produced no separation. It is shown in Figure S7 of the Supporting Information that racemic proline can clearly be resolved with *L*-Pro-COMS ($\alpha_{D/L} = 6.26 \pm 1.98$) and, to a lesser extent, with *L*-Ile-COMS ($\alpha_{D/L} = 1.14 \pm 0.01$) and even with *L*-His-COMS, where a small degree of reverse enantiodiscrimination ($\alpha_{D/L} = 0.92$) can be observed. It is worth mentioning that *DL*-Pro-COMS produced no separation of racemic proline as was expected for a nonchiral solid. These results suggest that the higher the anisotropy measured by polarized Raman spectroscopy (see Figure S8 of the Supporting Information comparing the four different *L*-AA-COMS) the better the separation. On the other hand, it seems that the chemistry of the amino acid, e.g., in terms of hydrogen bonding with silica hydroxyls and acid–base

properties, plays a key role in transferring chirality to the silica. At the working pH, the proportion of the anionic form of the amino acid is lower for arginine ($pK_{a3} = 12.48$) than for the others. This translates into a lack of electrostatic interaction during the synthesis of COMS between the micelle and the amino acid, in agreement with a lower optical sensitivity (see Figure S6 of the Supporting Information for the Raman spectra of *L*- and *DL*-Arg-COMS) and the absence of enantiomeric selectivity in *L*-Arg-COMS. Another issue deals with what is called in the synthesis of zeolites the hydrophobic hydration: organic compounds that have no hydrophobic hydration sphere do not organize silica.⁴¹ In terms of the interaction with silica required for the chirality transfer, this idea would favor the use of proline and isoleucine with side chains of lower polarity than those in histidine and arginine.

Proline gives rise to the best results in terms of both imprint and racemic resolution. Proline is the only proteinogenic amino acid possessing a naturally restricted conformation characterized by the presence of a pyrrolidine ring in which the N–C bond is inserted. In consequence, the chiral and quite rigid proline ring, not present in the other three amino acids, would be responsible for the enantioselective interaction with the efficient COMS. Additionally, *L*-AA-COMSs other than *L*-Pro-COMS do not discriminate the corresponding amino acid (AA) used in the silica synthesis. This fact suggests that our calcined COMS are not “tailor-made” solids as other chiral imprinted materials, but true chiral ordered silicas. The cavities formed in the silica are pores with a tridimensional backbone structure with a specific handedness, induced by the amino acid, that remains even after calcination. In addition, conformationally restricted proline is the best chirality inductor for chiral silica synthesis, and *L*-Pro-COMS is consequently the most enantioselective material obtained here. In fact, *L*-proline is a versatile organocatalyst able to induce high enantioselectivities in a number of useful organic transformations, as Manich and aldol reactions.⁴²

With the aim of checking the chiral nature of our calcined COMS, its circular dichroism (CD) properties were measured. Because of the lack of UV absorption of the COMS, induced circular dichroism (ICD) was carried out on calcined *L*-Pro-COMS, the material that showed the highest enantiodiscrimination ability. This technique is based on the circular dichroism measurement of the asymmetry induced by a chiral environment on an achiral molecule.⁴³ Here, phenol was identified as the appropriate achiral probe.

For comparison, and to prevent misleading results coming from artifacts, ICD was also studied on calcined *D*-Pro-COMS and *DL*-Pro-COMS. These solids were obtained in the same *L*-Pro-COMS synthesis conditions but using *D*-Pro and *DL*-Pro, respectively, instead of *L*-Pro. Figure 4 shows the CD spectra obtained in the ICD experiments on the three mentioned Pro-COMS solids. The location of the ICD signal appears in the wavelength region corresponding to achiral chromophore phenol (about 270 nm). The ICD signals for both *L*-Pro-COMS and *D*-Pro-COMS are of similar intensity but opposite value. It can, therefore, be concluded that the chiral handedness of *L*-Pro-COMS is opposite to that of *D*-Pro-COMS, as expected for a pair of enantiomers. On the other hand, the spectrum of *DL*-Pro-COMS shows no ICD signal. These observations point directly to the chiral nature of *L*-Pro-COMS and *D*-Pro-COMS.

In addition, Figure 5 displays the electron microscopy data recorded on the calcined *L*-Pro-COMS completing the previous TEM characterization shown in Figure 2 and Figure S3 of the

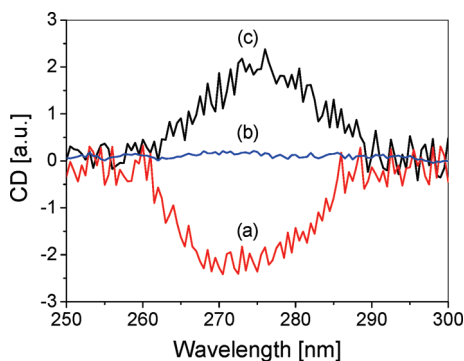


Figure 4. Solid-state ICD spectra corresponding to calcined samples after phenol adsorption: (a) L-Pro-COMS, (b) DL-Pro-COMS, and (c) D-Pro-COMS.

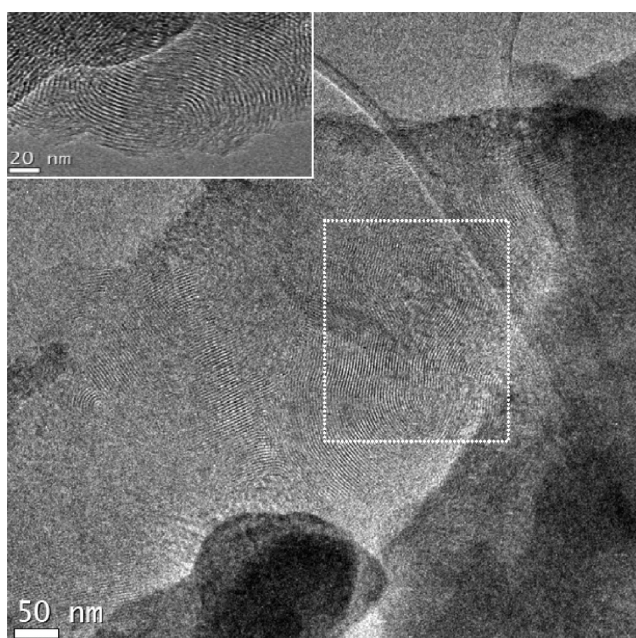
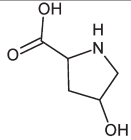
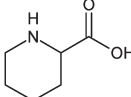
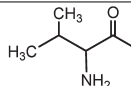
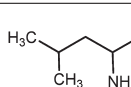
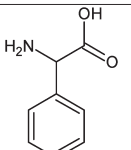


Figure 5. TEM micrograph of the calcined material showing the different orientation of the mesopores, which may induce the chirality. “Eight-like” domain is marked by the dashed square, while the inset corresponds to a different particle.

Supporting Information. The thin particle presents a well-defined pore arrangement, typical of these materials, but with random pore orientations. The dashed region and inset in Figure 5 show sites where the pores change their direction resembling an “eight-like” morphology. This could be related to the enantioselectivity observed in these materials and to the especial Raman and ICD features. The change in orientation in these domains takes place on a dimension closer to the pore size and the molecule diameter than in other helical mesostructured materials, exhibiting chirality on a scale about 2 orders of magnitude larger than the mesopore size.¹⁵

Once the chirality of calcined L-Pro-COMS was evidenced, this solid was used to treat other racemic solutions besides those of the amino acids involved in the synthesis of COMS. Two cyclic amino acids (trans-4-hydroxyproline and pipercolic acid) and two branched chain hydrophobic amino acids (valine and leucine) were chosen by structural analogy with proline and isoleucine, respectively. The unusual amino acid 2-phenylglycine was also

Table 3. Enantiomeric Separation Factors Resulting from Shaking Calcined L-Pro-COMS with Various Racemic Mixtures^a

| Racemic solution | Structural formula | D/L-racemate separation factor ($\alpha_{D/L}$) |
|------------------------------|--|---|
| Proline (Pro) | (see Table 2) | 6.26 ± 1.98 (3) |
| Isoleucine (Ile) | (see Table 2) | 1.30 ± 0.18 (2) |
| trans-4-Hydroxyproline (Hyp) |  | 0.70 ± 0.08 (3) |
| Pipercolic acid |  | 1.51 ± 0.04 (2) |
| Valine (Val) |  | 1.09 ± 0.05 (2) |
| Leucine (Leu) |  | 1.12 (1) |
| Phenylglycine (Phg) |  | 1.15 ± 0.03 (2) |

^a In the case of the $\alpha_{D/L}$ value, the figure between brackets corresponds to the number of repeated experiments with a powder of L-Pro-COMS obtained from a different synthesis batch.

tested as an example of an acyclic amino acid with a conformationally restricted structure around the α carbon. As shown in Table 3, all the new amino acids were resolved on L-Pro-COMS. The best resolutions were achieved with cyclic amino acids ($\alpha_{D/L}$ was 0.70 and 1.51 for trans-4-hydroxyproline and pipercolic acid, respectively). Despite the structural similarity between proline and trans-4-hydroxyproline, it is worth noting that reverse enantiodiscrimination can be observed on L-Pro-COMS. This fact again points to a chiral silica at structural level and not to the effect of a chiral organic residue present in the material. Acyclic amino acid resolutions, even that of the more conformationally restricted 2-phenylglycine, were lower than that of isoleucine ($\alpha_{D/L}$ was 1.09, 1.12, and 1.15 for valine, leucine, and 2-phenylglycine, respectively), possibly because isoleucine has two stereogenic centers. The resolution of different amino acids, none of which was used for the imprint procedure, demonstrates that L-Pro-COMS can be of broad application, in particular in the chromatographic field.

CONCLUSIONS

The combination of tetraethyl orthosilicate and quaternized aminosilane (with a templating role) silica sources with amino acids led to the synthesis of chiral ordered mesoporous silica (COMS), exhibiting enantioselectivity after calcination. Among the amino acids tested, proline gave rise to the best material (Pro-COMS) in terms of both imprint and racemic resolution of the

different racemates studied. The chiral and quite rigid proline ring, not present in the other three amino acids tested (arginine, histidine, and isoleucine), would be responsible for that. Even though conventional morphologies such as helices observed in other analogous materials are not reported, some of the characterizations carried out here (Raman spectroscopy, induced circular dichroism (ICD), and TEM) are compatible with a material singularly featured. Furthermore, ICD allows one to conclude that Pro-COMS is a chiral inorganic material, where the handedness of L-Pro-COMS is opposite to that of D-Pro-COMS, as expected for a pair of enantiomers, while the spectrum of DL-Pro-COMS shows no ICD signal. These observations together with the resolution of several racemates confirm the chiral nature of calcined L-Pro-COMS.

Even though arginine, histidine, isoleucine, and proline are different in terms of side chain polarity and hydrophobicity index, all of them give rise to ordered mesoporous silica. This suggests that the experimental procedure used in this research is flexible enough for probable application to most of the standard amino acids and to other kinds of chiral organic compounds as chirality inductors. This would open up new possibilities for multitude of applications involving, among others, asymmetric catalysis and enantiomeric separation.

■ ASSOCIATED CONTENT

S Supporting Information. Experimental data on ^{29}Si MAS NMR, TEM imaging, N_2 adsorption/desorption isotherms, and Raman spectra. This material is available free of charge via the Internet at <http://pubs.acs.org>.

■ AUTHOR INFORMATION

Corresponding Author

*E-mail: coronas@unizar.es.

■ ACKNOWLEDGMENT

Financial support from the Spanish Ministry of Science and Innovation (MAT2007-61028) is gratefully acknowledged. C.C. also acknowledges a "Juan de la Cierva" grant from the Spanish Science and Innovation Ministry. María Savirón is thanked for HPLC-MS analysis. In addition, the authors thank Prof. Avelino Corma, Prof. Miguel Menéndez, Prof. José Antonio Mayoral, Prof. Michael Tsapatsis, and Prof. Fernando Rey for fruitful discussions.

■ REFERENCES

- (1) Kumar, P.; Gulianti, V. V. *Microporous Mesoporous Mater.* **2010**, *132*, 1–14.
- (2) Boveri, M.; Aguilar-Pliego, J.; Perez-Pariente, J.; Sastre, E. *Catal. Today* **2005**, *107–08*, 868–873.
- (3) Vallet-Regi, M.; Ramila, A.; del Real, R. P.; Perez-Pariente, J. *Chem. Mater.* **2001**, *13*, 308–311.
- (4) Li, X. X.; Barua, S.; Rege, K.; Vogt, B. D. *Langmuir* **2008**, *24*, 11935–11941.
- (5) Pedernera, M.; de la Iglesia, O.; Mallada, R.; Lin, Z.; Rocha, J.; Coronas, J.; Santamaria, J. J. *Membr. Sci.* **2009**, *326*, 137–144.
- (6) Melde, B. J.; Johnson, B. J.; Charles, P. T. *Sensors* **2008**, *8*, 5202–5228.
- (7) Kresge, C. T.; Leonowicz, M. E.; Roth, W. J.; Vartuli, J. C.; Beck, J. S. *Nature* **1992**, *359*, 710–712.
- (8) Zhao, D.; Huo, Q.; Feng, J.; Chmelka, B. F.; Stucky, G. D. *J. Am. Chem. Soc.* **1998**, *120*, 6024–6036.
- (9) Wan, Y.; Zhao, D. Y. *Chem. Rev.* **2007**, *107*, 2821–2860.
- (10) Yokoi, T.; Yoshitake, H.; Tatsumi, T. *Chem. Mater.* **2003**, *15*, 4536–4538.
- (11) Che, S.; Garcia-Bennett, A. E.; Yokoi, T.; Sakamoto, K.; Kunieda, H.; Terasaki, O.; Tatsumi, T. *Nat. Mater.* **2003**, *2*, 801–805.
- (12) Lee, S. B.; Mitchell, D. T.; Trofin, L.; Nevanen, T. K.; Söderlund, H.; Martin, C. R. *Science* **2002**, *296*, 2198–2200.
- (13) Okamoto, Y.; Ikai, T. *Chem. Soc. Rev.* **2008**, *37*, 2593–2608.
- (14) Clark, L. A.; Chempath, S.; Snurr, R. Q. *Langmuir* **2005**, *21* (6), 2267–2272.
- (15) Fan, J.; Boettcher, S. W.; Tsung, C.-K.; Shi, Q.; Schierhorn, M.; Stucky, G. D. *Chem. Mater.* **2008**, *20* (3), 909–921.
- (16) Yokoi, T.; Iwama, M.; Watanabe, R.; Sakamoto, Y.; Terasaki, O.; Kubota, Y.; Kondo, J. N.; Okubo, T.; Tatsumi, T.; Ruren, Xu, Z. G. J. C.; Wenfu, Y. *Stud. Surf. Sci. Catal.* **2007**, *170* (2), 1774–1780.
- (17) Choi, S.; Coronas, J.; Jordan, E.; Oh, W.; Nair, S.; Okamoto, F.; Shantz, D. F.; Tsapatsis, M. *Angew. Chem., Int. Ed.* **2008**, *47*, 552–517.
- (18) Seral, J. J.; Uriel, S.; Coronas, J. *Eur. J. Inorg. Chem.* **2008**, *31*, 4915–4919.
- (19) Cha, J. N.; Stucky, G. D.; Morse, D. E.; Deming, T. J. *Nature* **2000**, *403*, 289–292.
- (20) Che, S.; Liu, Z.; Ohsuna, T.; Sakamoto, K.; Terasaki, O.; Tatsumi, T. *Nature* **2004**, *429*, 281–284.
- (21) Jin, H.; Liu, Z.; Ohsuna, T.; Terasaki, O.; Inoue, Y.; Sakamoto, K.; Nakanishi, T.; Ariga, K.; Che, S. *Adv. Mater.* **2006**, *18*, 593–596.
- (22) Coradin, T.; Duruphy, O.; Livage, J. *Langmuir* **2002**, *18* (6), 2331–2336.
- (23) Coradin, T.; Livage, J. *Colloids Surf., B* **2001**, *21* (4), 329–336.
- (24) Belton, D.; Paine, G.; Patwardhan, S. V.; Perry, C. C. *J. Mater. Chem.* **2004**, *14* (14), 2231–2241.
- (25) Davis, T. M.; Snyder, M. A.; Krohn, J. E.; Tsapatsis, M. *Chem. Mater.* **2006**, *18* (25), 5814–5816.
- (26) Yokoi, T.; Sakamoto, Y.; Terasaki, O.; Kubota, Y.; Okubo, T.; Tatsumi, T. *J. Am. Chem. Soc.* **2006**, *128*, 13664–13665.
- (27) Marx, S.; Avnir, D. *Acc. Chem. Res.* **2007**, *40* (9), 768–776.
- (28) Fireman-Shoresh, S.; Marx, S.; Avnir, D. *Adv. Mater.* **2007**, *19* (16), 2145–1450.
- (29) Fireman-Shoresh, S.; Popov, I.; Avnir, D.; Marx, S. *J. Am. Chem. Soc.* **2005**, *127*, 2650–2655.
- (30) Orfi, L.; Lin, M.; Larive, C. K. *Anal. Chem.* **1998**, *70* (7), 1339–1345.
- (31) Diaz, I.; Perez-Pariente, J. *Chem. Mater.* **2002**, *14* (11), 4641–4646.
- (32) Kruk, M.; Jaroniec, M.; Kim, J. H.; Ryoo, R. *Langmuir* **1999**, *15*, 5279–5284.
- (33) Huo, Q. S.; Margolese, D. I.; Stucky, G. D. *Chem. Mater.* **1996**, *8*, 1147–1160.
- (34) Luan, Z. H.; Meloni, P. A.; Czernuszewicz, R. S.; Kevan, L. *J. Phys. Chem. B* **1997**, *101*, 9046–9051.
- (35) Blin, J. L.; Carteret, C. *J. Chem. Phys. C* **2007**, *111*, 14380–14388.
- (36) Astorino, E.; Peri, J. B.; Willey, R. J.; Busca, G. J. *Catal.* **1995**, *157*, 482–500.
- (37) Haggmueller, R.; Gommans, H. H.; Rinzler, A. G.; Fischer, J. E.; Winey, K. I. *Chem. Phys. Lett.* **2000**, *330*, 219–225.
- (38) Rao, A. M.; Jorio, A.; Pimenta, M. A.; Dantas, M. S. S.; Saito, R. *Phys. Rev. Lett.* **2000**, *84* (8), 1820–1823.
- (39) Song, K.; Rabolt, J. F. *Macromolecules* **2001**, *34*, 1650–1654.
- (40) Lambert, J.-F. *Origins Life Evol. Biospheres* **2008**, *38*, 211–242.
- (41) Corma, A.; Davis, M. E. *Chem. Phys. Chem.* **2004**, *5*, 304–313.
- (42) Notz, W.; Tanaka, F.; Barbas, C. F., E. *Acc. Chem. Res.* **2004**, *37*, 580–591.
- (43) Fireman-Shoresh, S.; Marx, S.; Avnir, D. *J. Mater. Chem.* **2007**, *17*, 536–544.